[Frontiers in Bioscience, Landmark, 25, 683-698, Jan 1, 2020]

cPKCβII is significant to hypoxic preconditioning in mice cerebrum

Yan Lv[1,2], Zhichuan Lin[2], Dongguo Li[3], Song Han[1], Nan Zhang[1], Hongning Zhang[4], Junfa Li[1]

[1]Department of Neurobiology, School of Basic Medical Sciences, Capital Medical University, Beijing 100069, China, [2] Department of Neurology, Hainan Provincial General Hospital, Haikou 570311, China, [3]Department of Bioninformatics, School of Basic Medical Sciences and School of Biomedical Engineering, Capital Medical University, Beijing 100069, China,[4]Department of Pharmacology, School of Basic Medical Sciences and School of Biomedical Engineering, Capital Medical University, Beijing 100069, China

TABLE OF CONTENTS

1. ABSTRACT

Stroke causes significant morbidity and mortality worldwide, for which no satisfactory preventive option currently exists. Hypoxic preconditioning (HPC) is a protective strategy for cerebral ischemic stroke. To this end, we have identified, Conventional protein kinase C (cPKC)BetaII to play an important role in HPC. Pathway analysis and protein–protein interaction network building and functional proteomic exploration was used to identify 38 proteins in 6 Kyoto Encyclopedia of Genes and Genomes pathways that interact with cPKCBetaII in brains subjected to HPC. The role of the oxidative phosphorylation pathway was confirmed by experimental validation, and the

demonstration that the activity of the complex I and complex V and expression and activity of Ndufv2 and ATP5d was increased. Ndufv2 was co-localized with PKCBetaII in neurons rather than glial cells. Together, these data show that Ndufv2 and the oxidative phosphorylation pathway play an important role in cPKCBetaII-related HPC mediated signalling, likely as an adaptive neuroprotective mechanism.

2. INTRODUCTION

Sustained ischemic and hypoxic injuries lead to heart attack and stroke, one of the leading causes of morbidity and mortality in humans worldwide (1). Despite a great progress in understanding the pathophysiology of stroke, clinical trials on the pharmacological neuroprotective treatments have not yet shown a great promise (2-3). Hypoxic preconditioning (HPC) is an endogenous adaptive phenomenon, that offers protection against severe ischemic/hypoxic injury by introduction of brief episodes of a sub-lethal hypoxia (4- 6).

Multiple protein kinases including protein kinase C (PKC) and mitogen-activated protein kinase are involved in HPC (6-8). Among these, a cooperative set of kinases including conventional PKC (cPKC)βII, as well as a group of downstream molecules are involved in the cerebral cortices that were are subjected to HPC induced by asphyxia in mouse (9-12). We used proteomic technology together with bioinformatic methods to systematically and specifically identify cellular signalling transduction pathways and key molecules that participate in HPC (13-14). Functional proteomic technology has been used to elucidate the mechanisms that are involved in HPC and to screen cPKCβII-specific signalling mediators (5). The protein–protein interaction (PPI) network is an important explorative strategy that is currently used in the genome and proteomic studies (15-16). In this study, all the experimentally identified cPKCβII-interacting proteins were placed into a systematic PPI network to understand the complex cellular organization. Pathway enrichment was performed to screen a list of genes in a specific biological context by mapping genes to known Kyoto Encyclopedia of Genes and Genomes (KEGG) pathways (17-18). We used the PPI network KEGG pathway enrichment of the direct functional proteomic data to understand and trace the hub signalling pathway or modulus mediated by cPKCβII in the cerebral HPC. The highly pertinent pathways were experimentally validated.

3. MATERIALS AND METHODS

3.1. Animal models

An auto-hypoxia (acute and repetitive exposure to progressive hypoxia)-induced HPC mouse model was prepared as previously reported (5, 19). Experiments were conducted at room temperature (18° C–22° C) in adult male BALB/c mice weighing 18–22 g. All procedures undertaken in the current study were conducted according to the guidelines set by the Animal Care and Use Committee of Capital Medical University and consistent with the National Institutes of Health (NIH) Guide for the Care and Use of Laboratory Animals (NIH Publications No. 80-23). Briefly, mice were individually placed within a 125-mL airtight jar, which was filled with fresh air and sealed with a rubber plug to duplicate a progressive hypoxic environment. This procedure closely simulates the clinical conditions of ‘asphyxia’, exemplified by a combination of hypoxia and hypercarbia. Mice were removed immediately after the appearance of the first gasping signs an indicator of the endpoint of each hypoxic exposure), and the tolerance time and final oxygen concentration were recorded. A minimum of 30 min was allowed for recovery under normoxic conditions; then, the mice were switched to another hermetically sealed jar of the same volume. HPC group (35.6 ± 1.5 min for tolerance time, 3.8% ± 0.7% for finished oxygen concentration) were mice that were exposed to auto-hypoxia for four times. Mice placed in open jars for the same duration were used as normoxic controls.

The procedures for intra-cerebro-ventricular injections of the cPKCβII inhibitor LY333531 were performed under anaesthesia induced by pentobarbital sodium (0.6 g/kg) with isotonic saline as the solvent (8). The drug was administered according to those described previously (20). While under anaesthesia, animals were positioned in a stereotaxic frame and a cannula (28-gauge, stainless steel, inner diameter 0.18 mm, outer

diameter 0.36 mm) was lowered stereotaxically into the left cerebral ventricle to a position defined by the following coordinates:

- 0.5 mm posterior to bregma
- mm lateral to bregma
- 3.5 mm below the skull surface

To ascertain that the solutions were administered exactly into the cerebral ventricle, some mice were injected with 5 µL diluted (1:10) India ink, and their brains were macroscopically examined post sectioning. The accuracy of the injection technique was evaluated, and 95% of the injections were found to be accurate.

3.2. Profiling of cPKCβII-interacting proteins in HPC mouse cortex

We used functional proteomic techniques, such as co-immunoprecipitation (co-IP), two-dimensional gel electrophoresis, silver staining and image analysis that traditionally have been used to identify the differentially expressed cPKCβII-interacting proteins in the cytosol of the mouse cortices that were subjected to HPC (5, 19). Proteins (500 µg) from the cytosolic or particulate fractions of mouse cortices were immunoprecipitated using 2 µg anti-cPKCβII polyclonal antibody (Santa Cruz Biotechnology, Inc., Santa Cruz, CA, USA). After incubation for 3 h, protein G Sepharose was added for 12 h at 4°C and the mixture was centrifuged for 1 min at 12,000 ×*g*. To remove non-specific binding products, the immunoprecipitates were washed four times with immunoprecipitation buffer (0.5% NP-40, Tris-Cl pH 8.0, 0.15 M NaCl). For the control experiments, the anti-cPKCβII antibody was replaced with the same volume of immunoglobulin G. The co-immunoprecipitates were resolved in thiourea buffer (6 M urea, 2 M thiourea, 4% CHAPS) by two-dimensional gel electrophoresis or by sodium dodecyl sulphate–polyacrylamide gel electrophoresis (SDS-PAGE). An equal amount of protein from three independent experiments was pooled to reduce inter-mouse variation. Triplicate gels were run for each group to obtain statistical significance for protein differences. First-dimensional isoelectric focusing was performed on an Ettan IPGphor System using 11-cm immobilized pH gradient strips with a linear pH gradient from 3 to 11 (GE Healthcare, UK) to cover a wide range of cPKCβII-interacting proteins. Samples were loaded, and active rehydration was performed at 30 V for 12 h at 20°C. The conditions used were as follows: 200 V for 1 h; 500 V for 1 h; 1000 V for 1 h; 8000 V for 1 h, and 8000 V for 3 h. The strips were then equilibrated with a solution containing 6 M urea, 30% glycerol, 2% SDS, 50 mM Tris-Cl and 1% dithiothreitol at pH 8.8 for 15 min, and the strips were then treated with the same solution containing 4% w/v iodoacetamide instead of the dithiothreitol. The strips were over-layered onto 10% homogeneous polyacrylamide gels and electrophoresed at 20 mA per gel. Gels were stained using a silver staining kit (GE Healthcare) according to the manufacturer's instructions. Images were digitized with an image scanner and analyzed using ImageMaster TM 2D Platinum Software program, version 5.0 (GE Healthcare). All spots were analyzed for gel-to-gel comparison. The total density in a gel image was used to normalize each spot volume and minimize inter-gel variation. The amount of each protein spot was expressed in terms of its volume. To assess the quantitative variations in the protein spot volumes, the volumes were normalized as a percentage of the total volume of all the spots present in a gel. The average number of fold changes was calculated by carrying out three repeated experiments. cPKCβII-interacting proteins spots were excized, destained, alkylated and digested with trypsin. The measured tryptic peptide masses were searched for in the Swiss-Prot and NCBInr databases using the MASCOT search algorithm (Matrix Science, UK) for protein identification. Several restrictions were imposed with tryptic peptides as follows: cysteine carbamidomethylation as the variable modification; a maximum of one trypsin mis-cleavage was allowed; peptide mass tolerance was set to 0.2 Da and protein scores greater than 54 were significant ($P < 0.05$). The identified cPKCβII-interacting proteins were transferred to Entrez Gene ID for KEGG pathway analysis (http://www.ncbi.nlm.nih.gov/gene/term=).

3.3. PPI network analysis of cPKCβII signalling in cerebral cortices subjected to HPC

We further established a PPI network of cPKCβII-interacting proteins in the cerebral cortices subjected to HPC. We employed PPI networks from IntAct, MINT, DIP and HAPRD databases (21). All included data were extracted

from co-IP, pull-down, blueprint and yeast-hybridization experimental techniques. The co-IP proteomic technology used for cPKCβII-related proteins included direct, indirect and presumed interacting proteins. The PPI network was built as cPKCβII seed protein nodes. The clustering confidence was calculated to evaluate the connecting efficiency of nodes as transduction significance.

3.4. KEGG pathway analysis of HPC

KEGG pathway (18) enrichment analysis based on the hypergeometric distribution was employed to identify functional modules from a high-throughput dataset of cPKCβII-interacting proteins. Pathway enrichment analysis is based on the hypergeometric distribution paradigm. To explore the molecular function represented in the gene profile, DAVID Bioinformatics Resources (http://david.abcc.ncifcrf.gov/summary.jsp) were utilised to identify the KEGG pathways enriched with PKC genes. The web of DAVID 6.8 (https://david.ncifcrf.gov/) was used to analyse differentially expressed genes at a significance level of $P < 0.05$ (22).

3.5. Western blot analysis

We carried out Western blotting as previously described (23). Briefly, 35 µg of protein from the whole tissue homogenates of the mouse frontal cortices were subjected to SDS–PAGE (12% SDS gel) and transferred to a polyvinylidene fluoride membrane. The polyvinylidene fluoride membranes were blocked and then incubated for 3 h at room temperature with primary rabbit polyclonal antibodies against Ndufv2 (Santa Cruz Biotechnology), Atp5a1, Atp5b (Abcam Biotechnology, USA) or Atp5d (Interprotec Biotechnology, China) at a dilution of 1:1000. Following incubation with the appropriate secondary antibodies (Interprotec Biotechnology), the enhanced chemiluminescence kit (GE Healthcare) was used to detect the signals. The blots were re-probed with primary monoclonal antibodies against β-actin (Sigma-Aldrich Company, USA) to verify equal loading of protein. Quantitative image analysis of Western blots was performed as previously reported (24). Immunoblotting was quantitatively analyzed after scanning the X-ray film using the Quantitative-One software program (Gel Doc 2000 imaging system, Bio-Rad Company, CA, USA). For determination of protein expression levels, the ratio (band density of protein/band density of β-actin) was expressed as 100% in the control group. Data from the other groups were expressed as a percentage of protein expression from the control group.

3.6. Isolation of mitochondria and assessment of activity of complex I and complex V

Mitochondria were isolated from the frozen mouse frontal cortices using the Mitochondrial Isolation Kit (Genmed Scientific Inc., Shanghai, China) and stored at −80°C. The activity of the complex I and complex were assayed using the Mitochondrial Function Kit (Genmed Scientific Inc.). Briefly after isolation of mouse cerebral mitochondria, the oxidation of reduced nicotinamide adenine dinucleotide (NADH) was recorded and the decrease in absorption was measured at 340 nm in the absence and presence of inhibitors (Genmed Scientifics Inc., Shanghai, China), specific for complex I (Rotenone) and V (Oligomycin). The activity ratios of complex I and complex were calculcated in the experimental gourp as a percentage by considering this value as being 100% in the control group.

3.7. Immunofluorescence analysis

As described previously, mice were anaesthetized with pentobarbital sodium (50 mg/kg, i.p.) and perfused transcardially with 0.1 M phosphate-buffered saline (PBS, pH 7.4) followed by 4% paraformaldehyde (24). The frontal cortices were post-fixed with the same fixative for at least 4 h at 4°C and was subsequently washed with PBS. The samples were then cryoprotected in serially diluted sucrose solution in PBS (10%, 20% and 30%), embedded in Tissue-Tek OCT compound (Sakura Finetek, Torrance, CA) and vertically cryosectioned, at a thickness of 16 µm, using a cryostat (Leica CM1850, Germany). Cryosections were collected onto coated slides, pre-incubated in PBS containing 5% bovine serum

albumin and 0.5% Triton X-100 for 1 h at room temperature and then incubated, overnight at 4º C, with one of the primary rabbit polyclonal antibodies against Ndufv2 at a dilution of 1:200. Following multiple rinses with PBS, the sections were incubated for 2 h in secondary antibodies or a mixture for double immunolabeling. The secondary antibodies used were rhodamine-labelled goat anti-mouse immunoglobulin G (red, Jackson Immuno Research, West Grove, PA) at a dilution of 1:400. Control sections were subjected to the same procedure and materials, without being incubated with primary antibodies. The sections were then cover-slipped in a mounting medium containing neuronal nuclei (NeuN) or glial fibrillary acidic protein (GFAP) (Vector Laboratories, Burlingame, CA) to visualize cell nuclei (green). Fluorescent sections were viewed by a confocal laser-scanning microscope (Leica TCS SP2, Germany). The images were captured with a Leica microscope imaging system (Leica, Wetzlar, Germany). Three selected fields in three serial sections were analyzed under a confocal laser-scanning microscope t 10×20 magnification, and the integrated densities of Ndufv2 and NeuN were analyzed by the ImageJ software program (NIH).

3.8. Statistical analysis

The data are presented as means ± standard errors. Statistical analysis was performed using one-way analysis of variance followed by pairwise multiple comparison procedures using the Bonferroni test. Differences with a P value of <0.05 were considered to be statistically significant.

4. RESULTS

4.1. Differentially expressed cPKCβII-interacting proteins in mouse cortices subjected to HPC

To explore the possible mechanism of cPKCβII-mediated neuroprotection, via a functional proteomic approach, we analyzed the brains of mice subjected to HPC and identified 38 proteins that interact with cPKCβII (Table 1).

4.2. PPI network analysis of cPKCβII signalling in HPC

To examine signal transduction and functional networks more closely, multi-step interactome analysis was further employed. The cPKCβII seeded PPI network (Figure 1) is comprised of 74 protein nodes, including interacting proteins plotted by proteomic methods and those revealed by experimental protein relations via analysis of the PPI network databases. 14-3-3β (Ywhab) is another efficient signalling molecule that, after HPC, it interacts with both the cPKCβII and OXPHOS molecules (Figure 1) (33).

4.3. KEGG pathway enrichment analysis of cPKCβII-interacting proteins

Pathway enrichment analysis is a canonical procedure that screens the key pathways from high-throughput data. In the current study, the 38 identified cPKCβII-interacting proteins were placed into the KEGG pathway dataset. The results indicated that cPKCβII-interacting proteins were enriched in six KEGG pathways (Table 2), including three neurodegenerative disease pathways involved in Parkinson's disease, Alzheimer's disease and Huntington's disease ($P < 0.05$), two cellular function pathways of gap junction and oxidative phosphorylation (OXPHOS) ($P < 0.05$), a core metabolic and cellular process pathway, and one immune system pathway of antigen processing and presentation. cPKCβII-specific KEGG pathway enrichment analysis showed that five proteins, including Ndufv2, Atpa1, Atp5b, Atp5d and Atp5h, were enriched in the OXPHOS (Figure 1).

4.4. HPC induces cPKCβII-specific changes in expression and activity of complex I and complex V proteins

The results revealed that OXPHOS was a key cPKCβII-interacting protein-enriched pathway. To explore the role of cPKCβII-interacting proteins in the OXPHOS, we examined the amount and

Table 1. Proteomic profiling of cPKCβII-interacting proteins in cerebral cortex of HPC mice

No	Protein name	Accession number	Gene symbol	Gene ID	Score	Matched peptides	Sequence coverage	Theoretical MW (Da)	Theoretical PI
1	14-3-3 protein gamma	P61982	Ywhag	22628	75	9	39%	28,285	4.8
2	78 kDa glucose-regulated protein precursor ???	P20029	Hspa5	14828	100	16	36%	72,377	5.07
3	Acetyl-CoA acetyltransferase, mitochondrial precursor	Q8QZT1	Acat1	110446	100	11	43%	44,787	8.71
4	Actin, cytoplasmic 1	Q6ZWM3	Actg1	11465	121	16	63%	41,710	5.29
5	Actin, cytoplasmic 2	P63260	Capza2	12343	114	13	49%	41,766	5.31
6	Alpha-enolase	P17182	Eno1	13806	138	15	50%	47,111	6.37
7	Alpha-internexin	P46660	Ina	226180	94	13	35%	55,708	5.23
8	ATP synthase subunit alpha, mitochondrial precursor ④	Q03265	Atp5a1	11946	58	9	23%	59,716	9.22
9	ATP synthase subunit beta, mitochondrial precursor ④	Q3U774	Atp5b	11947	159	20	61%	56,265	5.19
10	ATP synthase subunit delta, mitochondrial	Q9DCX2	Atp5d	66043	72	8	50%	18,738	5.52
11	Ceramide glucosyltransferase	O88693	Ugcg	22234	55	5	26%	45,436	7.94
12	Clathrin light chain B ???	Q6IRU5	Cltb	74325	64	8	33%	25,156	4.56
13	Cysteine-rich hydrophobic domain 1 protein ???	Q8CBW7	Chic1	12212	59	8	46%	25,774	4.56
14	Dihydrolipoyllysine-residue acetyltransferase component of pyruvate dehydrogenase complex, mitochondrial precursor	Q8BMF4	DLAT	1737	57	12	18%	67,899	8.81
15	Dihydropyrimidinase-related protein 2 (Collapsin response mediator protein-2, CRMP-2)	O08853	Dpysl2	12934	125	15	43%	62,239	5.95
16	Glial fibrillary acidic protein	Q7TQ30	Gfap	14580	71	13	42%	49,870	5.27
17	Glutamine synthetase	P15105	Glul	14645	139	16	48%	42,092	6.64
18	Glyceraldehyde-3-phosphate dehydrogenase	Q569X5	Gapdhs	14447	60	8	46%	35,787	8.44
19	Guanine nucleotide-binding protein G (I)/G (S)/G (T) subunit beta-1	P62874	Gnb1	14688	85	11	50%	37,353	5.6
20	Guanine nucleotide-binding protein G (I)/G (S)/G (T) subunit beta-2	P62880	Gnb2	14693	91	12	55%	37,307	5.6
21	Heat shock cognate 71 kDa protein ???	Q3U9G0	Hspa8	15481	59	10	20%	70,827	5.37

contd...

Table 1. Contd...

No	Protein name	Accession number	Gene symbol	Gene ID	Score	Matched peptides	Sequence coverage	Theoretical MW (Da)	Theoretical PI
22	Heat shock-related 70 kDa protein 2 ???	P17156	Hspa2	15512	57	8	19%	69,983	5.58
23	Heterogeneous nuclear ribonucleoproteins A2/B1	O88569	Hnrnpa2b1	53379	67	9	28%	37,380	8.97
24	NADH dehydrogenase (ubiquinone) flavoprotein 2, mitochondrial precursor ④	Q9D6J6	Ndufv2	72900	61	6	40%	27,610	7
25	Neurofilament light polypeptide	P08551	Nefl	18039	67	10	26%	61,471	4.62
26	Nipped-B-like protein	Q6KCD5	Nipbl	71175	66	17	9%	315,253	8.09
27	Pyruvate dehydrogenase E1 component subunit beta, mitochondrial precursor	Q9D051	Pdhb	68263	79	10	44%	38,912	6.41
28	SET domain-containing protein 4	P58467	Smyd4	319822	57	8	30%	49,805	9.33
29	Sushi domain-containing protein 2 precursor	Q9DBX3	Susd4	96935	55	10	23%	90,583	6.17
30	Transgelin-3	Q9R1Q8	Tagln3	56370	95	10	51%	22,456	6.84
31	Tripartite motif-containing protein 56	Q80VI1	Trim56	384309	54	9	22%	79,463	8.31
32	Tropomodulin-2	Q9JKK7	Tmod2	50876	60	8	33%	39,487	5.28
33	Tryptophanyl-tRNA synthetase, cytoplasmic	P32921	Wars	22375	54	7	23%	54,323	6.44
34	Tubulin alpha-1C chain ???	P68373	Tuba1c	22146	156	19	60%	49,877	4.96
35	Tubulin beta-2A chain ???	Q7TMM9	Tubb2a	22151	233	26	66%	49,875	4.78
36	Ubiquitin carboxyl-terminal hydrolase isozyme L1 ???	Q9R0P9	Uchl1	22223	60	7	41%	24,822	5.14
37	Ufm1-specific protease 1	Q9CZP0	Ufsp1	70240	55	6	41%	23,405	6.22
38	Vimentin	P20152	Vim	22352	63	11	27%	53,655	5.06
For relevance with latter KEGG pathway analysis, ???, ??? and ??? represent one, two and four enriched KEGG pathways participated by the cPKCβII-interacting protein, respectively.									

activity of respiratory complex I and complex V proteind in the cortex of mice after they were subjected to HPC.The activity of the complex I was significantly higher ($P < 0.05$, n = 9 per group) in the HPC group as compared to the normoxic control group; an effect that could be abolished in presence of cPKCβII inhibitor LY333531 (Figure 2).

Similarly, Western blot analysis demonstrated that Ndufv2 protein expression increased after HPC, and LY333531 blocked the increased protein expression of Ndufv2 as compared with the HPC groups ($P < 0.05$, n = 6 per group, Figure 3). No changes were observed in the levels of ATP5a, ATP5b or ATP5d.

4.5. Cellular localization of Ndufv2 in HPC

Ndufv2 exhibited cPKCβII-related changes in terms of amount and activity after mice were subjected to HPC. Immunolocalization of Ndufv2 showed that it was higher in neurons in the cortex

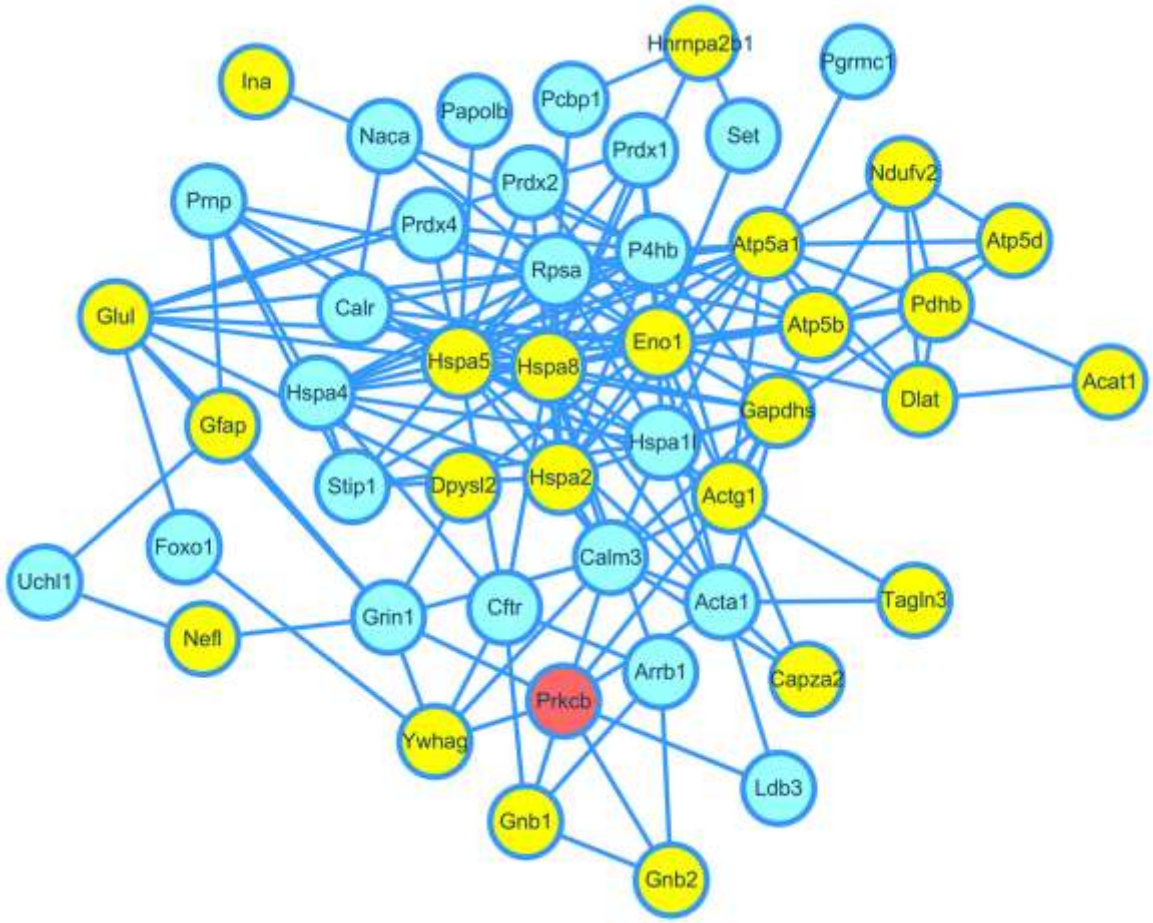

Figure 1. PPI network analysis of cPKCβII signaling in HPC. The red circle represented the seed protein as cPKCβII (Prckb), the yellow circles represented differentially expressed cPKCβII-interacting proteins, the blue circles represented the assumed interacting proteins.

Table 2. Enriched KEGG pathways of cPKCβII-interacting proteins in cerebral cortex of HPC mice

	Pathways	P Value	Genes
KEGG pathways	mmu05012: Parkinson's disease	0.001734	Ndufv2, Atp5a1, Atp5b, Atp5d, Uchl1
	mmu05016: Huntington's disease	0.00551	Ndufv2, Atp5a1, Atp5b, Atp5d, Cltb
	mmu00190: Oxidative phosphorylation	0.014449	Ndufv2, Atp5a1, Atp5b, Atp5d, Atp5h
	mmu05010: Alzheimer's disease	0.034869	Ndufv2, Atp5a1, Atp5b, Atp5d
	mmu04540: Gap junction	0.045827	Prkcb, Tubb2a, Tuba1c
	mmu04612: Antigen processing and presentation	0.05073	Hspa2, Hspa5, Hspa8

after exposure to HPC as compared to the cortex subjected to normoxia and this increase was blocked by the addition of cPKCβII inhibitor LY333531 (Figure 4A). However, the integrated density of Ndufv2 and NeuN between groups failed to achieve statistical significance (Figure 5). Moreover, Ndufv2 was absent in GFAP$^+$ glial cells (Figure 4B).

5. DISCUSSION

cPKCβII was identified to play an important role in HPC and by use of functional

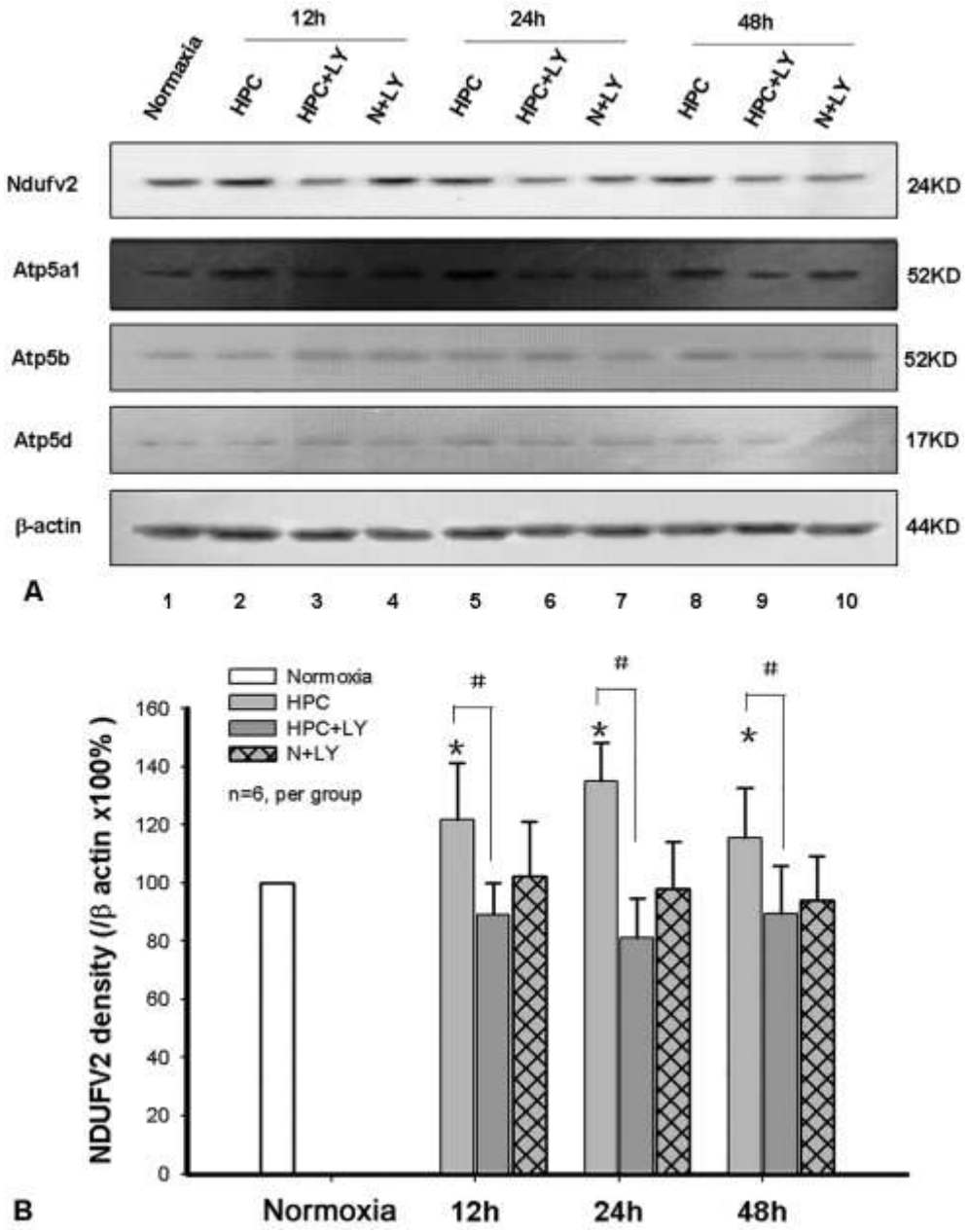

Figure 2. Ndufv2, Atp5a1, Atp5b, and Atp5d levels in HPC. A. Typical Western blot result of levels of OXPHOS proteins (Ndufv2, Atp5a1, Atp5b, and Atp5d) in HPC. B. Quantitative analysis Ndufv2 changes in HPC (*P < 0.05 vs. normoxia, #P < 0.05 vs. HPC group, n=6 per group).

proteomic exploration in the cortices subjected to HPC, we identified that cPKCβII interacts with a set of differentially expressed interacting proteins. Although proteomic and genomic studies have become progressively more widely used in studies involving signal transduction, co-IP matrix-assisted laser desorption/ionisation time-of-flight (MALDI-TOF) mass spectrometry (MS)-based functional proteomic research has rarely been used in studies involving kinases. We used pathway analysis and protein–protein interaction network building and functional proteomic

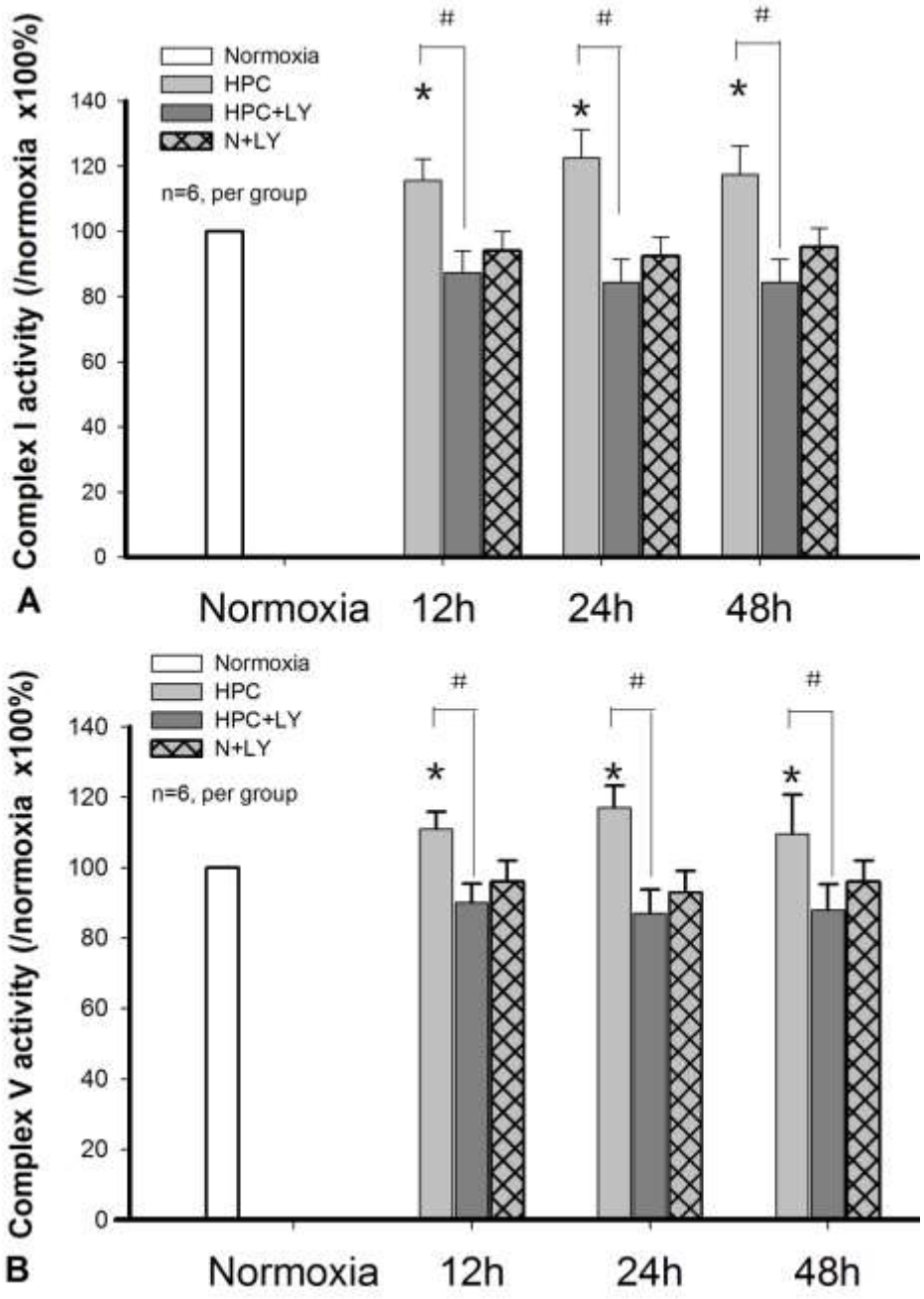

Figure 3. OXPHOS Complex I and V changes during HPC. A. Complex I activity changes in HPC in a cPKCβII-dependent manner (*P < 0.05 vs. normoxia group, #P < 0.05 vs. HPC group, n=6 per group). B. Complex V activity changes in HPC in a cPKCβII-dependent manner (*P < 0.05 vs. normoxia, #P < 0.05 vs. HPC group, n=6 per group).

exploration to identify 38 proteins in 6 Kyoto Encyclopedia of Genes and Genomes pathways that interact with cPKCBetaII in brains that were subjected to HPC. This approach has advantages and limitations when compared with other similar methods, such as those involving protein kinase

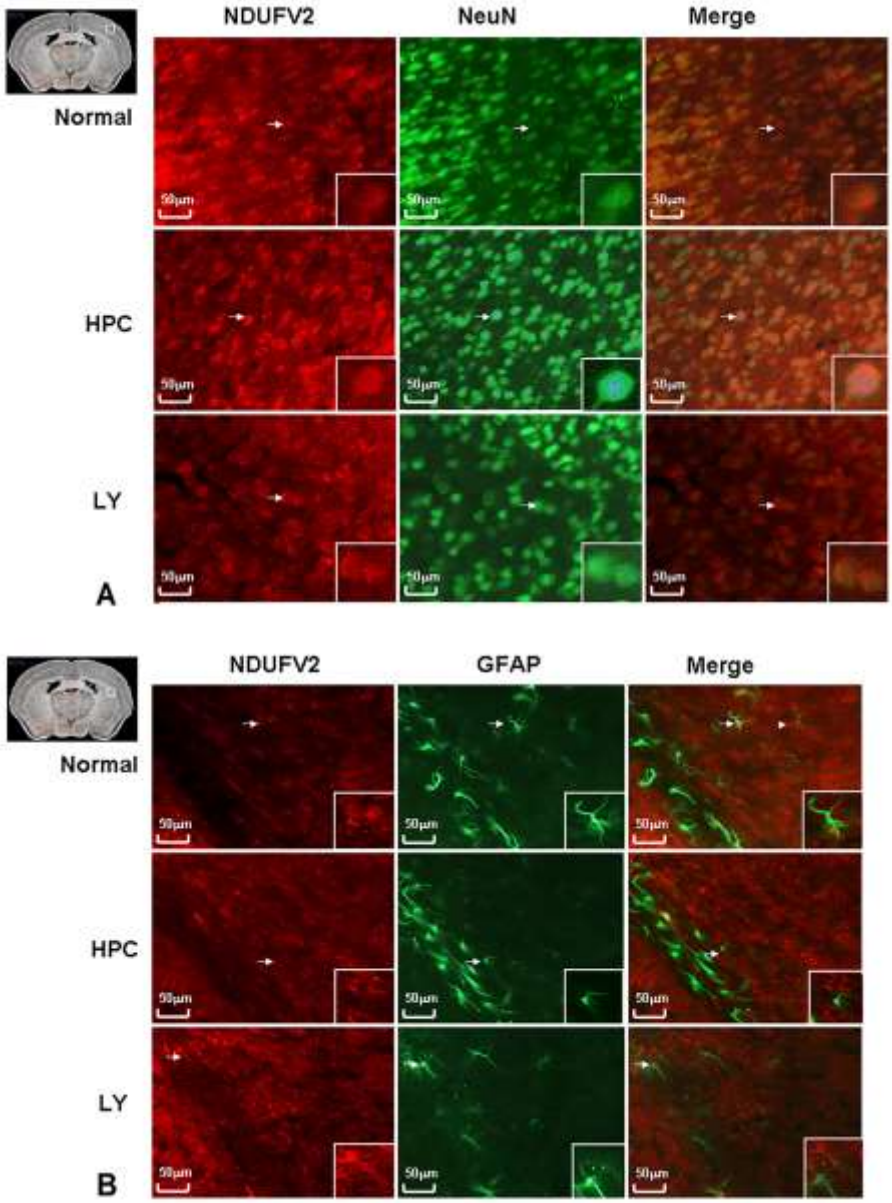

Figure 4. Immunofluorescence of Ndufv2 in HPC. Since NDUFV2 showed cPKCβII related changes in protein expression level and mitochondrion complex function level in HPC, we further employed immunohistochemical staining to test the functional cellular localisation of Ndufv2. Ndufv2 increased in HPC compared with normal mice cortex, and the increase could be blocked by LY333531 (Figure 4 A). Meanwhile, the NDUFV2 did not present in glial cells where GFAP were stained (Figure 4 B).

inhibitors or the RNAi method (25-26). The priority of this frame is to plot interacting proteins with high affiliations, such as a bait protein in HPC, which would bring congruity and more specific circumscription for the pathway and PPI analysis. This method is limited by its inability to identify the post-transcriptional modifications of the interactions, such as phosphorylation. However, this limitation might be compensated for by the diversity of the interactome.

Pathway analysis is an integrated method

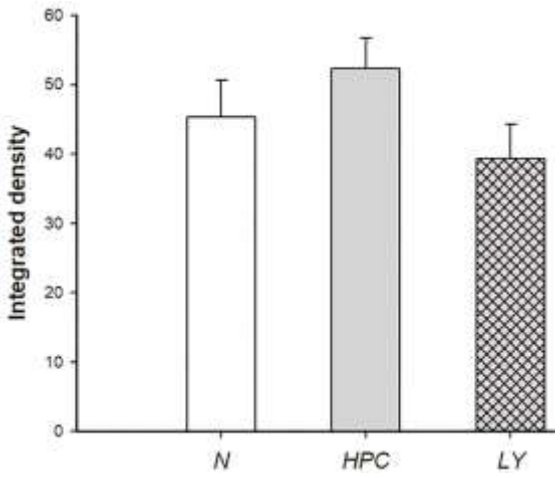

Figure 5. Integrated Immunofluorescence density of Ndufv2 and NeuN in HPC. The integrated density of Ndufv2 and NeuN between groups showed Ndufv2 increased in HPC compared with normal mice cortex, and the increase could be blocked by LY333531. However, the changes between groups failed to achieve statistical significance.

involving prior knowledge of the statistical method of hypergeometric distribution. We selected this method to directly process the functional proteomic data of cPKCβII plotted proteins involved in HPC, and 6 significant KEGG pathways were screened. In agreement with previous studies, results show that cPKCβII modulates the OXPHOS. KATPase on the outer membrane of mitochondria is a well-established preconditioning target (27). The lack of ATP generation can influence enzyme activities, molecular transport and membrane integrity under hypoxic or ischemic conditions (27). During OXPHOS, NADH, generated from glycolysis and the citrate (KREBS) cycle, are passed to oxygen via a chain of electron carriers. The OXPHOS has been shown to directly or indirectly influence apoptosis by its impact on KATPase and release of cytochrome C (28-29). The activity of the main components of OXPHOS, namely, complexes I, II and IV, increases in hearts that are subjected to ischemic preconditioning, and this increase is due to an increase in phosphorylation by nPKCε (30). PPI network analysis also indicated that the proteins involved in OXPHOS acquire dominant topological characteristics.

Among the 38 cPKCβII-interacting proteins identified in the mouse cerebral cortices subjected to HPC, Ndufv2 was found to be highly up-regulated. We experimentally validated the changes in the OXPHOS in the cerebral cortices that were subjected to HPC and showed that the activity of the complex I and complex V and expression and activity of Ndufv2 and ATP5d were increased in a cPKCβII-dependent manner. This is consistent with recent results indicating that cPKCβ shows a significant, rapid and long-lasting increase in mitochondria and influences generation of reactive oxygen species (ROS) and production of ATP after ischemia in the CA2–CA4 and DG regions of the hippocampus (31-32). Ndufv2 is a key subunit of complex I, whereas Atpa1, Atp5b, Atp5d and Atp5h are subunits of complex V (33). The relationship between OXPHOS, especially of Ndufv2, and cPKCβII indicates their potential role as a target in ischemia. Ndufv2 was colocalized with PKCBetaII in neurons rather than $GFAP^+$ glial cells. Ndufv2 was higher in cortical neurons in mice that were subjected to HPC than in cortical neurons of normal mice , and such increase was blocked by LY333531.

However, given that chronic ischemia and hypoxia occur in neurodegenerative diseases, in addition to the OXPHOS, other pathways that participate in HPC include those involved in Parkinson's disease, Huntington's disease, Alzheimer's disease, and pathways of antigen processing and presentation (34-36). Topological analysis of the network revealed that 14-3-3β (Ywhab), which is related both to cPKCβII and OXPHOS as another candidate molecule involved in HPC (33). 14-3-3β is an effector molecule that interacts with cPKCβII and its downstream OXPHOS to offer a protective role in cerebral preconditioning.

6. ACKNOWLEDGMENTS

This work was supported by the following grants: National Natural Science Foundation of China (30871219, 31071048 and 31171147), China 973 Pre-program (2011CB512109), Ph.D. Programs Foundation of Ministry of Education of China (20091107110001) and the Funding Project for

Academic Human Resources Development in Institutions of Higher Learning under the Jurisdiction of Beijing Municipality (PHR200906116).

7. REFERENCES

1. McCoy CE, Langdorf MI, Lotfipour S: American Heart Association/American Stroke Association Deletes Sections from 2018 Stroke Guidelines. West J Emerg Med 19 (6), 947-951 (2018).
DOI: 10.5811/westjem.2018.9.39659

2. Kernan WN, Ovbiagele B, Black HR, Bravata DM, Chimowitz MI, Ezekowitz MD, Fang MC, Fisher M, Furie KL, Heck DV: Guidelines for the prevention of stroke in patients with stroke and transient ischemic attack: a guideline for healthcare professionals from the American Heart Association/American Stroke Association. Stroke 45 (7), 2160-2236 (2014).
DOI: 10.1161/STR.0000000000000024

3. Messe SR, Gronseth G, Kent DM, Kizer JR, Homma S, Rosterman L, Kasner SE: Practice advisory: Recurrent stroke with patent foramen ovale (update of practice parameter): Report of the Guideline Development, Dissemination, and Implementation Subcommittee of the American Academy of Neurology. Neurology 87 (8), 815-821 (2016).
DOI: 10.1212/WNL.0000000000002961

4. Wakai T, Narasimhan P, Sakata H, Wang E, Yoshioka H, Kinouchi H, Chan PH: Hypoxic preconditioning enhances neural stem cell transplantation therapy after intracerebral hemorrhage in mice. J Cereb Blood Flow Metab 36 (12), 2134-2145 (2016).
DOI: 10.1177/0271678X15613798

5. Bu X, Zhang N, Yang X, Liu Y, Du J, Liang J, Xu Q, Li J: Proteomic analysis of cPKCbetaII-interacting proteins involved in HPC-induced neuroprotection against cerebral ischemia of mice. J Neurochem 117 (2), 346-356 (2011).
DOI: 10.1111/j.1471-4159.2011.07209.x

6. Liu C, Peng Z, Zhang N, Yu L, Han S, Li D, Li J: Identification of differentially expressed microRNAs and their PKC-isoform specific gene network prediction during hypoxic pre-conditioning and focal cerebral ischemia of mice. J Neurochem 120 (5), 830-841 (2012).
DOI: 10.1111/j.1471-4159.2011.07624.x

7. Li J, Niu C, Han S, Zu P, Li H, Xu Q, Fang L: Identification of protein kinase C isoforms involved in cerebral hypoxic preconditioning of mice. Brain Res 1060 (1-2), 62-72 (2005).
DOI: 10.1016/j.brainres.2005.08.047

8. Wei H, Li Y, Han S, Liu S, Zhang N, Zhao L, Li S, Li J: cPKCgamma-Modulated Autophagy in Neurons Alleviates Ischemic Injury in Brain of Mice with Ischemic Stroke Through Akt-mTOR Pathway. Transl Stroke Res 7 (6), 497-511 (2016).
DOI: 10.1007/s12975-016-0484-4

9. Wakai T, Narasimhan P, Sakata H, Wang E, Yoshioka H, Kinouchi H, Chan PH: Hypoxic preconditioning enhances neural stem cell transplantation therapy after intracerebral hemorrhage in mice. J Cereb Blood Flow Metab 36 (12), 2134-2145 (2016).
DOI: 10.1177/0271678X15613798

10. Stetler RA, Leak RK, Gan Y, Li P, Zhang F, Hu X, Jing Z, Chen J, Zigmond MJ, Gao Y: Preconditioning provides neuroprotection in models of CNS disease: paradigms and clinical

significance. Prog Neurobiol 114, 58-83 (2014).
DOI: 10.1016/j.pneurobio.2013.11.005

11. Stangherlin A, O'Neill JS: Signal Transduction: Magnesium Manifests as a Second Messenger. Curr Biol 28 (24), R1403-R1405 (2018).
DOI: 10.1016/j.cub.2018.11.003

12. Kapupara K, Wen YT, Tsai RK, Huang SP: Soluble P-selectin promotes retinal ganglion cell survival through activation of Nrf2 signaling after ischemia injury. Cell Death Dis 8 (11), e3172 (2017).
DOI: 10.1038/cddis.2017.566

13. Chen X, Zhang X, Jia C, Xu J, Gao H, Zhang G, Du X, Zhang H: Membrane depolarization increases membrane PtdIns (4,5)P2 levels through mechanisms involving PKC betaII and PI4 kinase. J Biol Chem 286 (46), 39760-39767 (2011)
DOI: 10.1074/jbc.M111.289090

14. Collins CJ, Chang IJ, Jung S, Dayuha R, Whiteaker JR, Segundo G, Torgerson TR, Ochs HD, Paulovich AG, Hahn SH: Rapid Multiplexed Proteomic Screening for Primary Immunodeficiency Disorders From Dried Blood Spots. Front Immunol 9, 2756 (2018).
DOI: 10.3389/fimmu.2018.02756

15. Quan Z, Quan Y, Wei B, Fang D, Yu W, Jia H, Quan W, Liu Y, Wang Q: Protein-protein interaction network and mechanism analysis in ischemic stroke. Mol Med Rep 11 (1), 29-36 (2015).
DOI: 10.3892/mmr.2014.2696

16. Thakur Z, Dharra R, Saini V, Kumar A, Mehta PK: Insights from the protein-protein interaction network analysis of Mycobacterium tuberculosis toxin-antitoxin systems. Bioinformation 13 (11), 380-387 (2017).
DOI: 10.6026/97320630013380

17. Wang J, Zheng W, Qian Y, Liang J: A Seed Expansion Graph Clustering Method for Protein Complexes Detection in Protein Interaction Networks. Molecules, 22 (12), E 2179 (2017).

18. Kanehisa M, Furumichi M, Tanabe M, Sato Y, Morishima K: KEGG: new perspectives on genomes, pathways, diseases and drugs. Nucleic Acids Res 45 (D1), D353-D361 (2017).
DOI: 10.1093/nar/gkw1092

19. Zhang N, Yin Y, Han S, Jiang J, Yang W, Bu X, Li J: Hypoxic preconditioning induced neuroprotection against cerebral ischemic injuries and its cPKCgamma-mediated molecular mechanism. Neurochem Int 58 (6), 684-692 (2011).
DOI: 10.1016/j.neuint.2011.02.007

20. Munoz A, Nakazaki M, Goodman JC, Barrios R, Onetti CG, Bryan J, Aguilar-Bryan L: Ischemic preconditioning in the hippocampus of a knockout mouse lacking SUR1-based K (ATP) channels. Stroke 34 (1), 164-170 (2003).
DOI: 10.1161/01.STR.0000048215.36747.D1

21. Rezaei-Tavirani M, Rezaei-Taviran S, Mansouri M, Rostami-Nejad M, Rezaei-Tavirani M: Protein-Protein Interaction Network Analysis for a Biomarker Panel Related to Human Esophageal Adenocarcinoma. Asian Pac J Cancer Prev 18 (12), 3357-3363 (2017)

22. Shen S, Kong J, Qiu Y, Yang X, Wang W, Yan L: Identification of core genes and outcomes in hepatocellular carcinoma by bioinformatics analysis. J Cell Biochem,

(2018).
DOI: 10.1002/jcb.28290

23. Feng S, Li D, Li Y, Yang X, Han S, Li J: Insight into hypoxic preconditioning and ischemic injury through determination of nPKCepsilon-interacting proteins in mouse brain. Neurochem Int 63 (2), 69-79 (2013).
DOI: 10.1016/j.neuint.2013.04.011

24. Zhao L, Liu X, Liang J, Han S, Wang Y, Yin Y, Luo Y, Li J: Phosphorylation of p38 MAPK mediates hypoxic preconditioning-induced neuroprotection against cerebral ischemic injury via mitochondria translocation of Bcl-xL in mice. Brain Res 1503, 78-88 (2013).
DOI: 10.1016/j.brainres.2013.01.051

25. Zhang N, Gao G, Bu X, Han S, Fang L, Li J: Neuron-specific phosphorylation of c-Jun N-terminal kinase increased in the brain of hypoxic preconditioned mice. Neurosci Lett 423 (3), 219-224 (2013)
DOI: 10.1016/j.neulet.2007.07.028

26. Qu Y, Shi X, Zhang H, Sun W, Han S, Yu C, Li J: VCAM-1 siRNA reduces neointimal formation after surgical mechanical injury of the rat carotid artery. J Vasc Surg 50 (6), 1452-1458 (2009).
DOI: 10.1016/j.jvs.2009.08.050

27. Thuc LC, Teshima Y, Takahashi N, Nagano-Torigoe Y, Ezaki K, Yufu K, Nakagawa M, Hara M, Saikawa T: Mitochondrial K (ATP) channels-derived reactive oxygen species activate pro-survival pathway in pravastatin-induced cardioprotection. Apoptosis 15 (6), 669-678 (2010).
DOI: 10.1007/s10495-010-0473-0

28. Kowalczyk JE, Kawalec M, Beresewicz M, Debski J, Dadlez M, Zablocka B: Protein kinase C beta in postischemic brain mitochondria. Mitochondrion 12 (1), 138-143 (2012).
DOI: 10.1016/j.mito.2011.06.002

29. Selvatici R, Marino S, Piubello C, Rodi D, Beani L, Gandini E, Siniscalchi A: Protein kinase C activity, translocation, and selective isoform subcellular redistribution in the rat cerebral cortex after *in vitro* ischemia. J Neurosci Res 71 (1), 64-71 (2003).
DOI: 10.1002/jnr.10464

30. Dave KR, DeFazio RA, Raval AP, Torraco A, Saul I, Barrientos A, Perez-Pinzon MA: Ischemic preconditioning targets the respiration of synaptic mitochondria via protein kinase C epsilon. J Neurosci 28 (16), 4172-4182 (2008).
DOI: 10.1523/JNEUROSCI.5471-07.2008

31. Alhazzani A, Rajagopalan P, Albarqi Z, Devaraj A, Mohamed MH, Al-Hakami A, Chandramoorthy HC: Mesenchymal Stem Cells (MSCs) Coculture Protects (Ca2+)i Orchestrated Oxidant Mediated Damage in Differentiated Neurons *In vitro*. Cells7 (12), (2018).

32. Lebuffe G, Schumacker PT, Shao ZH, Anderson T, Iwase H, Vanden HT: ROS and NO trigger early preconditioning: relationship to mitochondrial KATP channel. Am J Physiol Heart Circ Physiol284 (1), H299-H308 (2003).
DOI: 10.1152/ajpheart.00706.2002

33. Zhou XY, Hu DX, Chen RQ, Chen XQ, Dong WL, Yi CL: 14-3-3 Isoforms

Differentially Regulate NFkappaB Signaling in the Brain After Ischemia-Reperfusion. Neurochem Res 42 (8), 2354-2362 (2017).
DOI: 10.1007/s11064-017-2255-3

34. Antonov AV, Dietmann S, Mewes HW. KEGG spider: interpretation of genomics data in the context of the global gene metabolic network. Genome Biol 9 (12), R179 (2008).
DOI: 10.1186/gb-2008-9-12-r179

35. Zhang F, Niu L, Li S, Le W: Pathological Impacts of Chronic Hypoxia on Alzheimer's Disease. Acs Chem Neurosci 10(2), 902-909 (2018).

36. Lange JH, Niehaus I, Cegolon L: Does generalized hypo-oxygenation (hypoxia) allow endotoxin into the brain through the blood brain barrier, thus increasing the risk for Parkinson disease? Croat Med J 57 (4), 406-407 (2016).
DOI: 10.3325/cmj.2016.57.406

Abbreviations: cPKCβII: conventional protein kinase CβII; HPC: hypoxic preconditioning; PPI: protein-protein-interacion; KEGG: Kyoto Encyclopedia of Genes and Genomes; OXPHO pathway: phosphorylation pathway; NADH: reduction nionamide adenine dinucleotide; ROS: reactive oxygen species; GFAP: glial fibrillary acidic protein

Key Words: cPKCbetaII, HPC, Proteomic, OXPHO pathway, PPI network, Cellular Signal Transduction

Send correspondence to: Junfa Li, Department of Neurobiology, Beijing Institute for Neuroscience, Capital Medical University, #10 You An Men Wai Xi Tou Tiao, Beijing 100069, PR China, Tel: 8610-8391-1475, Fax: 8610-8395-0060, E-mail: junfali@ccmu.edu.cn